Separation Science and Technology
Publication details, including instructions for authors and subscription information:
http://www.informaworld.com/smpp/title~content=t713708471

Unified Analysis of Compressive Packed Beds, Filter Cakes, and Thickeners

George G. Chase[a]
[a] DEPARTMENT OF CHEMICAL ENGINEERING, THE UNIVERSITY OF AKRON, AKRON, OHIO

To cite this Article Chase, George G.(1992) 'Unified Analysis of Compressive Packed Beds, Filter Cakes, and Thickeners', Separation Science and Technology, 27: 8, 1093 — 1114
To link to this Article: DOI: 10.1080/01496399208019026
URL: http://dx.doi.org/10.1080/01496399208019026

SEPARATION SCIENCE AND TECHNOLOGY, 27(8 & 9), pp. 1093–1114, 1992

Unified Analysis of Compressive Packed Beds, Filter Cakes, and Thickeners

GEORGE G. CHASE
DEPARTMENT OF CHEMICAL ENGINEERING
THE UNIVERSITY OF AKRON
AKRON, OHIO 44325-3906

Abstract

Fluid–particle systems are widely used throughout industry. Using an *ad hoc* approach to model a particular fluid–solid process lacks generality. A unified approach using continuum theory for multiphase systems is applied here to evaluate a packed bed, filter cake, and continuous gravity thickener. The unified approach has the advantage that the governing equations are obtained by simplifying the generalized continuum equations. The simplifying assumptions are obvious from the equations and do not require intuitive understanding as does the *ad hoc* approach. Also, for similar localized conditions the same constitutive relations can be applied when the same material is used in several processes. In the packed bed, filter cake, and thickener modeled here, a compressible solid matrix behavior is represented by a truncated Taylor series expansion for the solid phase stress. The packed bed and filter cake behaviors are evaluated for a range of pump powers and bed masses or cake heights. The thickener behavior is evaluated for a range of feed and sludge discharge concentrations.

INTRODUCTION

Fluid–particle systems are widely used throughout industries to perform a variety of operations from fluid/solid separations to mass and heat transfer over extended surface areas. The design of such systems can be done empirically through trial and error and experimentation. However, a more cost effective approach is to apply theoretical stochastic or deterministic methods to reduce the costs of the experimentation.

Fluid–particle processes are highly complex, and our understanding of the mechanisms controlling the process behavior is incomplete. The traditional *ad hoc* approach to modeling such processes has provided governing equations for specific operations and have improved our understanding of those operations. Some disadvantages to the *ad hoc* approach are that the assumptions inherent in the derivation of the models may not be obvious, similarities between the processes are obscure and hinder transfer of information, and adaption of the models to compressive particulate phases may not be clear.

A "unified" approach is taken in this work in which the governing equations that model the significant affects of the processes are obtained from volume-averaged continuum theory. As can be expected, when done properly the same governing equations are obtained from either the *ad hoc* or unified approaches. However, in applying the unified approach the analysis is analogous to that used for single phase systems which makes it easier to understand and apply, the necessary assumptions become explicit, similarities between processes can be exploited, and material property behavior is always introduced through the constitutive functions.

The unified approach using the volume-averaged continuum theory also has the advantage that the general equations are derived directly from lower scale single phase equations which describe the individual phase behaviors. Furthermore, the general continuum equations provide an inventory of mechanisms controlling multiphase processes in general. Hence, less commonly known mechanisms, such as "virtual mass" in the momentum jump discontinuity for fluidized beds (*1*, *18*), can be accounted for and are less likely to be overlookead when obtaining the simplified governing equations.

To show how to apply the continuum theory to all multiphase processes would have too broad a scope. Hence the scope of this work is narrowed down to the isothermal processes of packed beds, filter cakes, and continuous gravity thickeners operating on the same compressible solid particulate material.

DESCRIPTION OF THE PROCESSES

The major features of the three processes are shown in Fig. 1. The packed bed is the simplest of the three processes. It has a bed made up of the particulate solids through which passes the fluid phase. The bed has a depth of length L, the pressure at the top of the bed is P_L, and the pressure at the bottom of the bed is P_0. The solid phase matrix is stationary when run at steady state, though it can have a nonuniform distribution of phases. This device is the simplest for determining empirical relations for the constitutive equations.

The filter cake is more complicated than the packed bed due to the solids content in the inlet slurry. The filter cake is inherently an unsteady process due to the change in cake height with respect to time, dL/dt. In contrast to the packed bed which has a stationary solid phase, the solid phase in

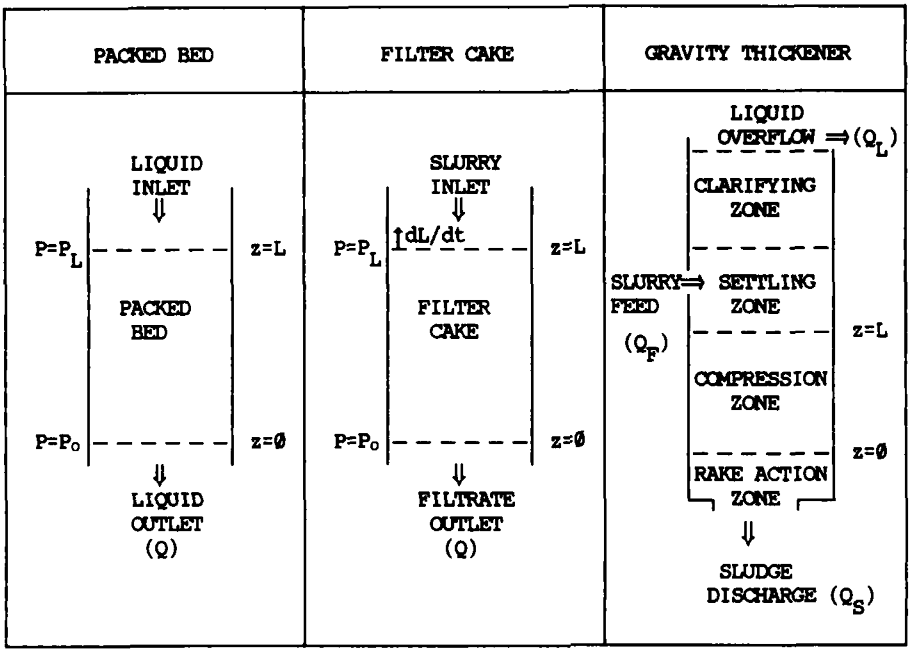

FIG. 1. Features of the packed bed, filter cake, and thickener processes.

the filter cake of a compressible solid moves slowly downward toward the filter medium at $z = 0$. The pressures at the top and bottom of the cake are denoted by P_L and P_0.

The filter medium at the bottom of the cake also has a pressure drop. This pressure drop is negelcted in this present work. However, it should be noted that there are situations, such as when the filter media clogs, in which this pressure drop can become significant.

For both the filter cake and the packed bed the primary driving force is due to the pressure drop. At steady state both the pressure drop and flow rate for the packed bed are constants (*17*). For the filter cake, typical experimental operations are run either at constant pressure or constant flow rate. Many industrial applications use centrifugal pumps to operate the filter cake, which results in a variable-pressure-variable-rate operation (*21*). This latter approach is modeled here for the packed bed and filter cake, in which the rate of work supplied by the pump, W, is taken to be a constant and is related to the pressure drop and flow rate by

$$W = Q\Delta P \tag{1}$$

The thickener is the most complicated of the three operations because it has several zones that interact. As shown in Fig. 1 these zones are the clarifying, settling, compression, and rake action zones. The two zones of primary interest are the settling and compression zones. In the settling zone the settling rate controls the rate at which the solids are separated out of the feed stream while in the compression zone the deformation of the solid matrix controls the solids concentration in the sludge outlet. In both of these zones, gravity is the driving force that causes the settling and deformation. The compression zone is most closely related to the packed bed and filter cake, except that it has a significant solid phase velocity.

Particles may settle in a fluid in several different manners (*19*), depending on the particle concentration (or volume fraction) and their relative tendency to cohere. At low concentrations, on the average, the particles are far apart and are free to settle individually. Collisions can occur between particles with different velocities. If upon collision the particles cohere, they can form floccules which will settle at their own characteristic rate.

In a more concentrated slurry the particles are more crowded together. The movement of the individual particles becomes hindered due to the flow fields of neighboring particles. The rate of movement of the particles under these conditions are referred to as hindered settling and can be related to the terminal velocity of the particles through an empirical correlation (*16*).

At some higher concentration (or volume fraction) the solid particles come into contact with each other and the solids matrix thus formed develops a compressive strength. The concentration at which this occurs is referred to as the "critical concentration" (*6*). Each layer of solids is able to provide mechanical support for the layers above. A given layer of solid matrix is compressed to concentrations above the critical concentration by the stresses acting on the layer. These stresses can be due to gravity or to the drag force (from a moving fluid phase) acting on the solid matrix above the given layer.

In a packed bed all of the solid particles are contained in the bed which is at or above the critical concentration. In cake filtration the cake itself is at or above the critical concentration. The slurry above the filter cake is below the critical concentration. Normally the flow rate in cake filtration is high enough that settling in the flurry above the cake can be neglected.

The flow rates in a thickener are inherently slower than cake filtration to allow settling to separate phases. The concentration of particles in the clarifying zone are typically low enough that the settling is unhindered. In the settling zone the particles settle by the hindered settling mechanism referred to above. In the compression zone, as it is being defined here, the concentration is at or above the critical concentration. For some materials there is a significant transition zone between the settling and compression zones in which the concentration varies with position. For the continuous thickener being evaluated here, this transition zone is not considered.

In all three processes, the bed, cake, and compression zones have a solid matrix of particles that have a compressive strength which is significantly less than the strength of the solid material itself. Under stress the solid particles may move relative to each other or, if the particles are fibrous, the fibers may bend and deform, which results in the movement and compression of the solid matrix. It is this compressive solid matrix to which the volume-averaged continuum theory is applied.

THE VOLUME-AVERAGED CONTINUUM EQUATIONS

Continuum theory provides us with a set of equations that describe the conservation laws of mass, momentum, energy, and entropy in a continuous material (*9*). These equations are derived independently of the material that makes up the system. Hence, these equations apply whether the system is a single or multiphase material or whether the fluids have Newtonian or non-Newtonian behavior. The material dependencies are accounted for in the constitutive relations.

For flows through porous media, in which there is considerable particle-to-particle contact to transmit forces and stresses, it is more appropriate to apply volume averaging to obtain continuum equations for each phase. These volume-averaged continuum equations explicitly account for the interactions between the phases.

The development of the volume-average continuum equations is reported in the literature (*2, 11–14, 20, 22*). There are a few subtle differences between some authors as to how the deviation terms are incorporated into the continuum equations. The point of view taken here is that of Hassanizadeh and Gray (*12*) who recognize that for most processes the deviation values cannot be experimentally separated from the other terms. Hence, the deviation terms are combined with the flux and internal energy expressions and are accounted for by the constitutive relations.

The continuum theory provides equations for the conservation of mass, momentum, energy, entropy, and the entropy generation. It is assumed here that the flows are isothermal and that all of the effects of interest are contained in the momentum and mass balances. Furthermore it is assumed that there are only two phases, fluid and solid, present in the system, and that there are no chemical reactions and no mass transfer between the phases.

Both phases are assumed to be intrinsically incompressible. For the solid phase this means that the individual solid particles do not compress under the loads experienced in the operations. However, the porous matrix at the volume-averaged scale is permitted to deform.

For the above conditions the mass and momentum balances are

α-Phase mass:

$$\frac{\partial}{\partial t}(\epsilon^\alpha \rho^\alpha) + \nabla\cdot(\epsilon^\alpha \rho^\alpha \mathbf{v}^\alpha) = 0, \qquad \text{for } \alpha = f, s \tag{2}$$

f-Phase momentum:

$$\frac{\partial}{\partial t}(\epsilon^f \rho^f \mathbf{v}^f) + \nabla\cdot(\epsilon^f \rho^f \mathbf{v}^f \mathbf{v}^f) + \epsilon^f \nabla P^f + \nabla\cdot\boldsymbol{\tau}^s - \epsilon^f \rho^f \mathbf{g} + \mathbf{F}^d = 0 \tag{3}$$

s-Phase momentum:

$$\frac{\partial}{\partial t}(\epsilon^s \rho^s \mathbf{v}^s) + \nabla\cdot(\epsilon^s \rho^s \mathbf{v}^s \mathbf{v}^s) + \epsilon^s \nabla P^f + \nabla\cdot\boldsymbol{\tau}^s - \epsilon^s \rho^s \mathbf{g} - \mathbf{F}^d = 0 \tag{4}$$

where the superscripts f and s indicate the fluid and solid phases, respectively. The superscripts α indicates either the fluid or solid phase. The terms in the mass balance, Eq. (2), account for mass accumulation and convection. The terms in the momentum balances, Eqs. (3) and (4), account for inertial, convective, pressure, stresses, gravity, and drag forces, respectively. The primary interaction between the two phases is the drag force, $\mathbf{F}^d$, which is due to a velocity difference between the phases. The chemical reaction and mass transfer terms have already been removed from Eqs. (2) through (4).

THE GOVERNING AND CONSTITUTIVE EQUATIONS

To evaluate the three processes, the continuum equations are simplified by assuming one-dimensional flow and by neglecting insignificant terms. A number of assumptions are made to simplify the mathematics to obtain the governing equations that account for the significant mechanisms controlling the processes. In the event there are materials and operating conditions for which these assumptions do not apply, then one would have to revise the assumptions and obtain the relevant governing equations.

The primary assumptions and the resulting simplified continuum equations are listed in Table 1 for comparison while the details of the evaluations are contained in the appendices.

TABLE 1
Assumptions and Simplified Continuum Equations

Assumptions Common to All Three Processes:

1. Isothermal operating conditions
2. One-dimensional flow
3. No chemical reactions or mass transfer
4. Dominant forces are pressure, gravity, drag, and solid matrix normal stress
5. Constant phase intrinsic densities, ρ^α

Simplified Equations

α-Phase mass: $$\frac{\partial}{\partial t}(\epsilon^\alpha) + \frac{\partial}{\partial z}(\epsilon^\alpha v_z^\alpha) = 0, \quad \text{where } \alpha = f,s \tag{5}$$

f-Phase momentum: $$\epsilon^f\frac{\partial \mathrm{P}}{\partial z} + F_z^d = 0, \quad \text{where } \mathrm{P} = P^f + \rho^f g \tag{6}$$

s-Phase momentum: $$\epsilon^s\frac{\partial \mathrm{P}}{\partial z} + \frac{\partial \tau_{zz}^s}{\partial z} + \epsilon^s(\rho^s - \rho^f)g - F_z^d = 0 \tag{7}$$

Assumptions Particular to the Operations

Packed bed	Filter cake	Gravity thickener
1. Steady state	1. Unsteady state	1. Steady state
2. Stationary solids	2. Solids velocity is much smaller than the fluid phase velocity	2. Settling solids rate given by hindered settling relation (*16*)
3. Pressure driving force provided by a centrifugal pump	3. Pressure driving force is provided by a centrifugal pump	3. Compression is due to solids weight in the compression zone
4. Neglect pressure losses due to fittings and end effects	4. Neglect pressure losses due to fittings and the filter medium	4. All solids exit through the sludge discharge stream
5. Neglect gravity force	5. Neglect gravity force	

Many of the assumptions are common to all three processes, resulting in the same three continuum relations, Eqs. (5)–(7), as the starting equations for the analysis in the appendices. Additional assumptions that only apply to a particular operation are also listed in Table 1. Most of the assumptions are self-explanatory. However, the fourth assumption, common to all three processes, may not be obvious. This assumption is based on dimensional analysis (*23*) and experimental verification (*5*) for the system behavior *at the volume-averaged continuum scale.* At a lower scale within the pores of the solid matrix the viscous shear and inertia forces are significant, but at the volume-averaged scale these forces have been averaged and are either accounted for in the drag force term or they are insignificant.

In all three operations the same constitutive relations are assumed for the drag force, F_z^d, and the solid phase normal stress, τ_{zz}^s, for the solids in the compressible solid matrix. We let the drag force be represented by the Blake–Kozeny expression (*3*) which is reformulated to the form

$$F_z^d = [B\mu A_s^2]\frac{\epsilon^{s2}}{\epsilon^f}(v_z^f - v_z^s) \tag{8}$$

Equation (8) shows that the drag force is proportional to the velocity difference between the phases. The specific surface area between the phases, A_s, is assumed to be a constant in the analysis, though for some materials it may change as a function of the normal stress on the solid phase matrix. For isothermal conditions the fluid phase intrinsic viscosity, μ, is a constant, and the parameter, B, is a material parameter of the multiphase mixture.

The solid phase normal stress in the z-direction is represented by

$$\tau_{zz}^s = \sigma(\epsilon^s - \epsilon_c^s) \tag{9}$$

which is the first-order term in a Taylor series expansion of the solids stress as a function of the strain (*4*). The modulus, σ, represents the rate of change of the stress with respect to the strain. The strain is represented by the difference in volume fractions, $(\epsilon^s - \epsilon_c^s)$, between position at z and the top of the bed (cake, or compression zone) where the interparticle contacts become just sufficient to transmit stress through the solid phase matrix.

The relation in Eq. (9) treats the solid matrix as an elastically compressible material (*15*). It only considers the normal stress in the z-direction which is consistent with the behavior of the three processes considered here. For more complex operations a more rigorous relation may be required to account for the nine components of the stress tensor (*9*, *10*).

MODELING RESULTS

The three operations are modeled here using the same constitutive relations and material parameters to emphasize the unified approach to multiphase systems. The material parameters used in the constitutive relations are estimated from preliminary experiments on fibrous cellulose particles in water and are listed in Table 2.

TABLE 2
Material Property and Operating Parameters Used in Modeling the Packed Bed, Filter Cake, and Thickener Processes

Material parameters for the drag and stress relations, Eqs. (8) and (9):

$$[B\mu A_s^2] = 9{,}530{,}000 \text{ kPa·s/m}^2, \quad \sigma = 3560 \text{ kPa}, \quad \epsilon_c^s = 0.12$$

Parameters for the hindered settling expression, Eq. (C.7):

$$u_t = 0.005 \text{ m/s}, \quad b = 5$$

Material intrinsic densities:

$$\rho^s = 1469 \text{ kg/m}^3, \quad \rho^f = 1000 \text{ kg/m}^3$$

Cross sectional area of packed bed and filter cake:	$A = 0.01$ m^2
Slurry solid phase volume fraction for filter cake:	$\epsilon^s_{\text{slurry}} = 0.04$

The values in Table 2 are applied to the equations derived in the appendices to obtain Fig. 2–7. These figures describe the behavior of the three processes as predicted by the governing equations under a range of operating conditions. These figures only depict the macroscale behavior of the overall processes. The local scale profiles of velocities, pressures, and volume fractions can also be determined from the equations but are not needed for this work.

Figures 2 and 3 show the behavior of a packed bed with a cross-sectional area of 0.01 m^2. In Fig. 2 the water flow rate through the packed bed is plotted versus the bed pressure drop for various pump powers and bed masses. This plot shows that the largest flow rates are obtained for the smaller bed masses. Conversely, the largest pressure drops are obtained for the larger bed masses. The pump power influences the degree to which the flow rate and pressure drop vary with bed mass.

For a compressible material the bed height will vary for a given bed mass. The bed height and flow rate are plotted in Fig. 3 as a function of bed pressure drop for two bed masses. The plot shows that as the pressure drop increases, the bed height decreases. The pump power is not shown on this plot but can be obtained from the flow rate and the pressure drop using Eq. (1).

Similar plots in Fig. 4 and 5 are obtained for a filter cake with a 0.01 m^2 cross-sectional area. In Fig. 4 the flow rate is plotted versus the cake pressure drop for varying pump power and cake heights. Early in the filtration when the cake height is small, most of the pump power is expended in producing the high flow rate. Late in the filtration when the

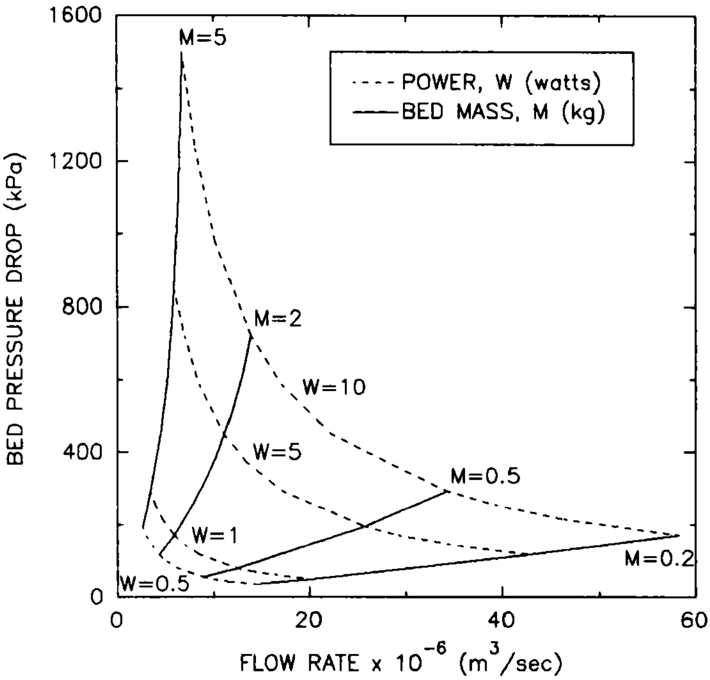

FIG. 2. Plot of flow rate and pressure drop for a packed bed for different bed solid phase masses and pump powers.

cake height is large, most of the pump power is dissipated across the cake as drag causing a large pressure drop. As with the packed bed, the pump power applied to the cake changed the degree to which the flow rate and pressure drop change for different cake heights.

Filtrations are inherently unsteady. It is advantageous to be able to estimate the time required to achieve a specified cake height, pressure drop, or flow rate. These quantities are plotted in Fig. 4 as a function of time for two different pump powers. As can be seen from the curves, a tenfold increase in the pump power yields roughly a tenfold increase in the cake pressure drop while the increase in cake height and flow rate is more moderate with time. In each case the pressure drop and cake height increase with time during the filtration while the flow rate decreases.

In Figs. 6 and 7 are plotted the results of modeling a thickener. In Fig. 6 the sediment height of the compression zone is ploted versus the feed flow rate per unit area of thickener. On this plot are the operating curves for constant feed and sludge discharge concentrations. Hence, if you know

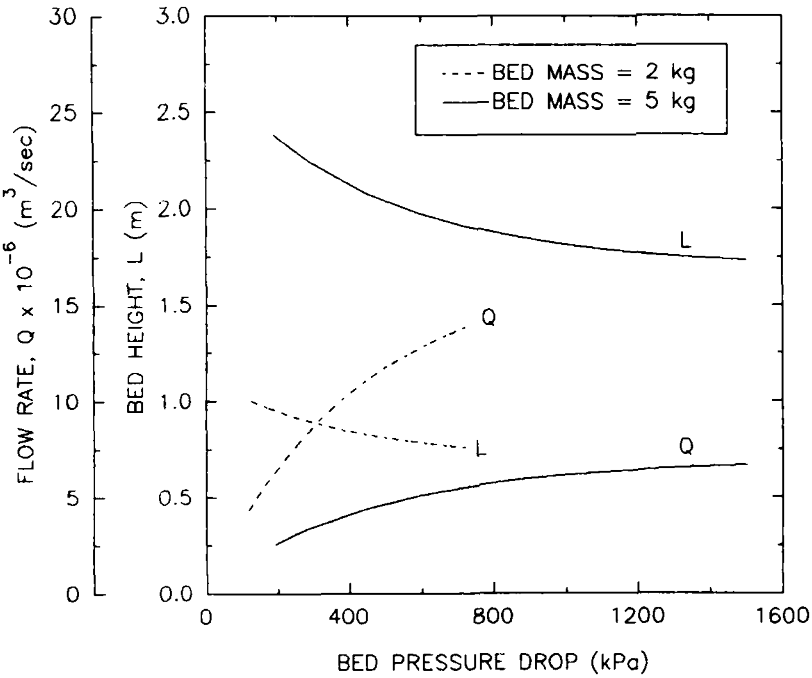

FIG. 3. Plot of flow rate and bed height as a function of bed pressure drop for two solid phase bed masses.

the feed rate and the concentrations of the feed and sludge discharge concentrations, then you can determine the height of the compression zone.

Operationally, the sludge discharge concentration is determined from the sludge discharge flow rate. The feed and discharge flow rates are plotted in Fig. 7 for various feed and discharge concentrations. Hence, between these two plots, with a given feed rate and feed concentration, the sludge discharge flow rate can be determined for a desired discharge concentration and the compression zone height can be estimated.

CONCLUSIONS

The unified approach using continuum theory for multiphase systems is applied here to the three processes of packed beds, cake filtration, and continuous gravity thickeners. The results show that the continuum scale governing equations can be determined for the three processes, and when the same material is used, then the same constitutive relations can be applied.

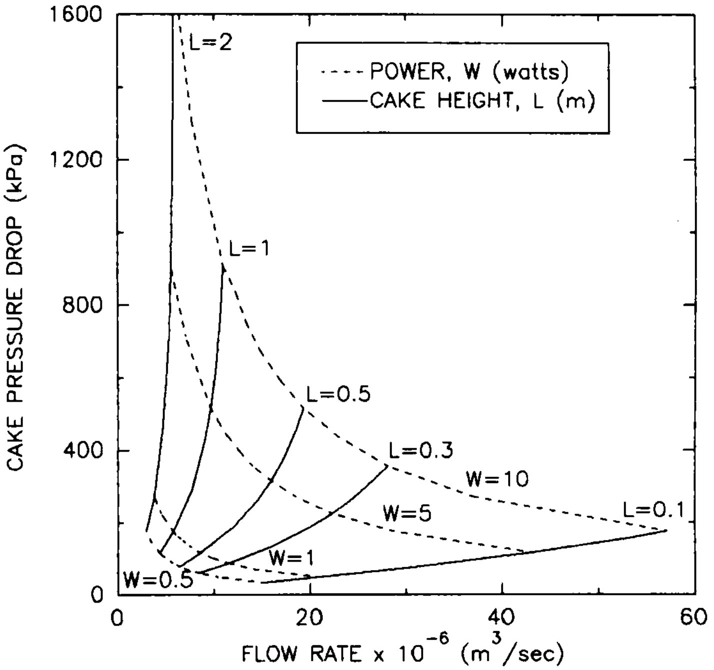

FIG. 4. Plot of filter cake pressure drop and flow rate for different pump powers and cake heights.

The packed bed is the simplest of the three operations. The modeling results show that for a constant bed mass the bed height varies with the flow rate and pressure drop with a compressible solid phase matrix.

The filter cake is more complex than the packed bed and requires additional calculations to relate the bed height to time. Since the cake pressure drop and flow rate are functions of the cake height then they can be determined as functions of time also.

The thickener is the most complex of the three processes, requiring a relation for the settling rate of particles in the settling zone. The calculations show that in principle, by controlling the feed and sludge discharge flow rates, the sludge discharge concentration and the sediment height of the compression zone can be controlled.

The approach used here may be used in modeling other multliphase processes, such as in expression in which a solid matrix is squeezed between two plates. Also, by removing assumptions and replacing terms removed from the equations, more complex operations can be evaluated. If other materials are to be used in a packed bed, filter cake, or thickener, the

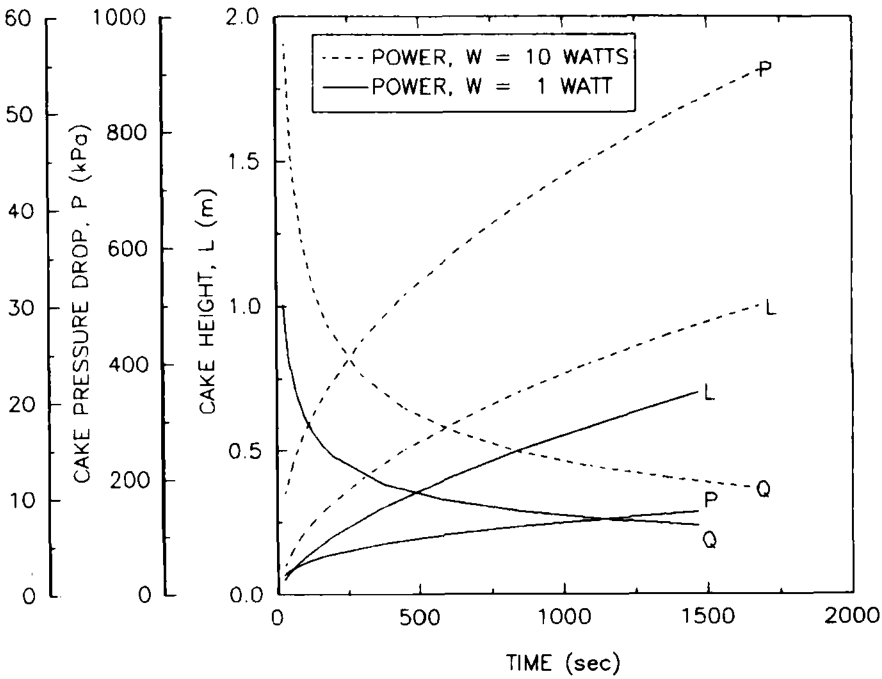

FIG. 5. Plot of filter cake pressure drop, flow rate, and cake height as a function of time for two different pump powers.

constitutive relations and parameter values can be replaced with those pertinent to the desired materials and the process behavior can be determined using the approach in this work.

APPENDIX A: PACKED BED EVALUATION

The assumptions in Table 1 are applied to Eqs. (1) and (5)–(9) in this appendix to evaluate packed bed behavior. The packed bed is the simplest of the three processes to evaluate. It has a liquid entering at the top of the bed and exiting at the bottom of the bed with the same flow rate, Q. For one-dimensional flow assumed here, the local continuum scale velocities are unifrom across the cross section of the packed bed. From the fluid phase mass balance, at steady state, the local velocitiy is related to the flow rate by

$$\epsilon^f v_z^f = -Q/A \qquad \text{(A.1)}$$

where A is the cross-sectional area of the packed bed and the minus sign accounts for the velocity in the minus z-direction.

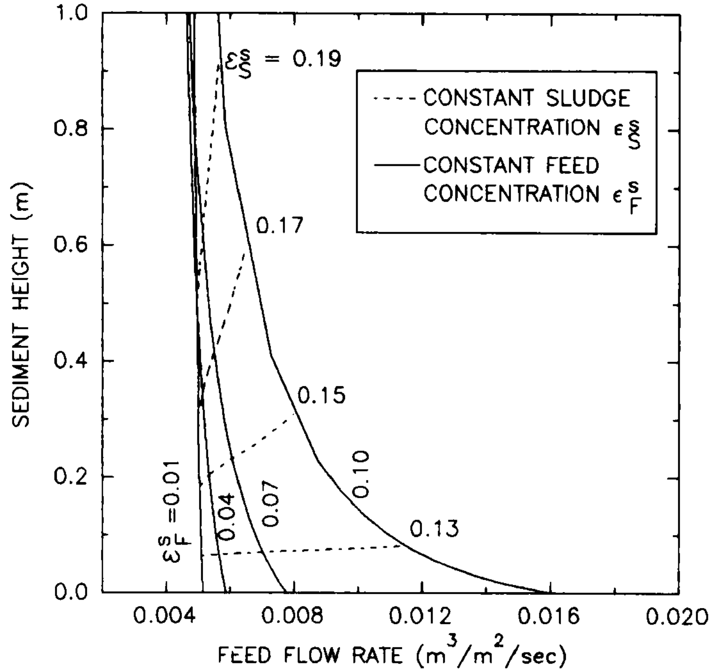

FIG. 6. Plot of feed stream flow rate and sediment height of the compression zone for the thickener for different feed and sludge stream concentrations.

Combining Eqs. (6)–(9) and (A.1), and neglecting the gravity term, gives

$$\frac{(1 - \epsilon^s)^3}{\epsilon^{s2}} \frac{d\epsilon^s}{dz} = - \frac{[B\mu A_s^2]Q}{\sigma A} \tag{A.2}$$

where the fluid phase volume fraction, ϵ^f, is changed into terms of the solid phase volume fraction by the identity $\epsilon^f + \epsilon^s = 1$. Equation (A.2) can be integrated to obtain

$$\left[\frac{1}{\epsilon^s} - \frac{1}{\epsilon_c^s}\right] + 3 \ln \left[\frac{\epsilon^s}{\epsilon_c^s}\right] + 3(\epsilon_c^s - \epsilon^s) + \frac{1}{2}(\epsilon^{s2} - \epsilon_c^{s2}) = - \frac{[B\mu A_s^2]}{\sigma} \frac{Q}{A} (L - z) \tag{A.3}$$

which relates the volume fraction to position. When evaluated at $z = 0$,

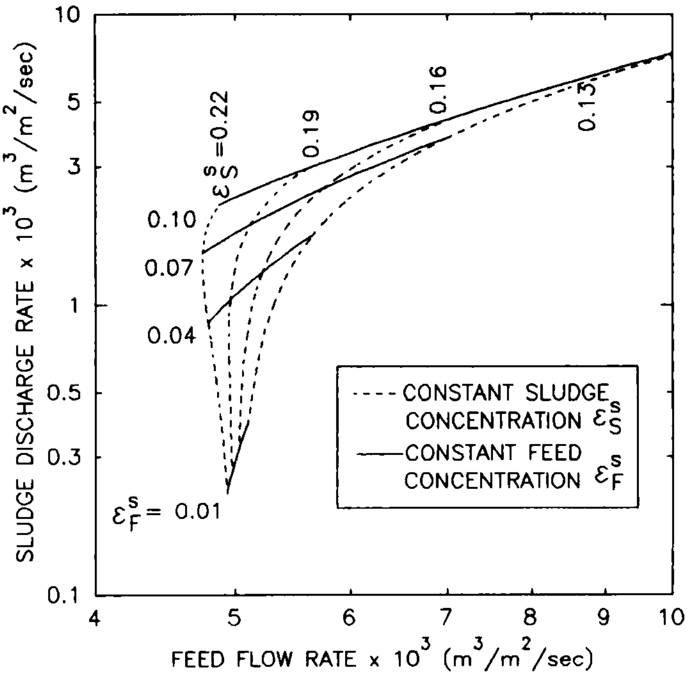

FIG. 7. Plot of feed and sludge discharge stream flow rates for the thickener for different feed and sludge stream concentrations.

this relates the volume fraction at the bottom of the bed, ϵ_0^s, to the bed height, L.

The pressure profile is obtained by combining Eqs. (6), (7), and (9), neglecting the gravity term, and integrating to obtain

$$P(L) - P(z) = \sigma(\epsilon^s - \epsilon_c^s) \tag{A.4}$$

When this equation is evaluated at $z = 0$, then the cake pressure drop is obtained:

$$\Delta P = P(L) - P(0) = \sigma(\epsilon_0^s - \epsilon_c^s) \tag{A.5}$$

Since the solid matrix is deformable, then for a given mass of solids, M^s, the bed height will vary with the stress. We can relate the total solid phase mass to the volume fractions at the top and bottom of the cake and the flow rate by

$$M^s = \rho^s A L \epsilon_{\text{bed}}^s \tag{A.6}$$

where ϵ^s_{bed} is the bed-averaged solid phase volume fraction. The bed-averaged volume fraction is given by

$$\epsilon^s_{bed} = \int_0^L \epsilon^s dz \tag{A.7}$$

which, through some mathematical manipulation, can be integrated to obtain

$$\epsilon^s_{bed} = \frac{-\sigma A}{[B\mu A_s^2]QL} \times \left[\ln\left[\frac{\epsilon^s_c}{\epsilon^s_0}\right] - 3(\epsilon^s_c - \epsilon^s_0) + \frac{3}{2}(\epsilon^{s2}_c - \epsilon^{s2}_0) - \frac{1}{3}(\epsilon^{s3}_c - \epsilon^{s3}_0)\right] \tag{A.8}$$

Hence, we get an expression for M^s by combining Eqs. (A.8) and (A.6). If we are given a mass of solid material, M^s, and the output power of the pump, W, we can then combine Eqs. (1), (A.5), (A.6), and (A.8) to determine the solid phase volume fraction at the bottom of the bed. Then, from the porosity profile, Eq. (A.3), it is possible to determine the total bed height.

APPENDIX B: FILTER CAKE EVALUATION

Cake filtration is very similar to the packed bed operation except that the amount of solid phase material in the cake increases over time. This makes cake filtration a moving boundary problem. The momentum balances, Eqs. (6) and (7), are implicitly dependent on time, while the mass balances, Eq. (5), are explicit. The moving boundary is accounted for in applying the mass jump balance conditions at the cake–slurry boundary.

Normally in cake filtration the velocity of the solid phase is insignificant compared to the fluid phase velocity. Hence the velocity difference in the drag force relation, Eq. (8), is approximated by

$$(v^f_z - v^s_z) = -Q/A\epsilon^f \tag{B.1}$$

The determination of the volume fraction and pressure profiles is identical to that for packed beds and are given by Eqs. (A.3) and (A.4).

Filter operations are normally terminated when either the pressure drop becomes too large (flow rate too small) or the cake height becomes too large (and the cake fills the filter assembly). For the variable-pressure-variable-rate filtration the pressure drop and flow rate are both functions of cake height. The cake height, in turn, varies with time. The cake height can be related to time through the mass balance.

To determine the cake height as a function of time, the fluid phase mass balance is combined with the mass jump balance at the top of the cake to obtain (*4*)

$$\frac{dL}{dt} = \frac{G(L)Q(L)}{A} \tag{B.2}$$

where $G(L)$ is a function of cake height, L, through the dependence of the cake average porosity, ϵ^f_{cake}, on L. The function $G(L)$ is given by

$$G(L) = \frac{1 - \epsilon^f_{slurry}}{\epsilon^f_{slurry} - \epsilon^f_{cake}} \tag{B.3}$$

where the fluid phase volume fraction of the slurry above the cake, ϵ^f_{slurry}, is assumed to be a constant and the cake average porosity is obtained from

$$\epsilon^f_{cake} = 1 - \epsilon^s_{cake} \tag{B.4}$$

and ϵ^s_{cake} is given in Eq. (A.8).

Equation (B.2) can be rearranged and integrated to obtain

$$\int_0^L \frac{A}{G(L)Q(L)} dL = t \tag{B.5}$$

which, when combined with Eqs. (1), (A.3), (A.5), (A.8), and (B.4), can be numerically integrated to relate cake height to time.

APPENDIX C: THICKENER EVALUATION

The thickener is the most complex of the three processes evaluated in this paper. A number of assumptions are used to reduce the equations to a more tractable form. The main assumptions are listed in Table 1. The thickener typically has several different zones or regions in which different mechanisms are important. It is assumed that all of the solids that enter the thickener exit through the sludge discharge. This means that only clear liquid exits at the top of the thickener. At the other end of the thickener the rake action in the rake action zone is assumed to only aid in moving the sludge through the cone-shaped opening at the bottom of the thickener and that it has no affect on the solids concentration in the slude discharge stream.

The two zones that have the greatest effect on the operation of the thickener are the settling and compression zones. In the settling zone the movement of the solid phase relative to the fluid phase is modeled using a hindered settling expression (*16*). In the compression zone the gravitational force causing the deformation can be related to the compression behavior of the solid matrix through the volume-averaged continuum equations.

Several equations can be deduced from the mass balances. Since the intrinsic densities are constant, they can cancel out of the phase mass balances, effectively yielding balances on the volumes for each phase. A balance over the whole thickener (i.e., at the macroscale) for steady state and constant intrinsic densities sets the feed stream volumetric flow rate equal to the sum of the flow rates exiting the thickener:

$$Q_F = Q_L + Q_S \tag{C.1}$$

Also, since all of the solid phase is assumed to exit through the discharge stream, a macroscale balance on the solid phase gives

$$\epsilon_F^s Q_F = \epsilon_S^s Q_S \tag{C.2}$$

while a balance on the liquid phase gives

$$\epsilon_F^f Q_F = \epsilon_S^f Q_S + Q_L \tag{C.3}$$

For the purposes of this evaluation, the volume-averaged velocities are assumed to be one-dimensional (plug flow) in the settling and compression zones. For large diameter thickeners and with appropriate slurry distributors at the feed inlet, this assumption is reasonable. However, if there are wall effects, turbulence, or other effects disrupting the flow, then this assumption would not hold.

At steady state the continuum scale mass balance gives

$$\frac{d}{dz}(\epsilon^\alpha v_z^\alpha) = 0 \tag{C.4}$$

which means that the product $\epsilon^\alpha v_z^\alpha$ is a constant, independent of the z-position in either the settling or compression zones. This product can be evaluated at $z = 0$ to obtain

$$\epsilon^s v_z^s = -\epsilon_S^s Q_S / A \tag{C.5}$$

$$\epsilon^f v_z^f = -\epsilon_S^f Q_S / A \tag{C.6}$$

where the minus signs account for the velocity vectors being in the minus z-direction. By combining Eqs. (C.2), (C.3), (C.5), and (C.6) then the products $\epsilon^\alpha v_z^\alpha$ can also be related to the feed inlet conditions.

Unlike the evaluations of the packed bed and the filter cake, in evaluating the thickener operation the velocity of the solid phase is significant. In the settling zone we assume that the movement of the solids is due to hidered settling. The hindered settling rate is given by (*16*)

$$u = u_t(\epsilon^f)^b \tag{C.7}$$

where u_t is the unhindered terminal velocity of the solids and b is a parameter that accounts for particle geometry, size, and Reynolds number. The velocity, u, is the average velocity of the solid particles relative to the fluid phase velocity.

$$u = -(v_z^s - v_z^f) \tag{C.8}$$

where u is a positive quantity and the minus sign accounts for the velocities in the minus z-direction.

Neglecting any zone transition effects and assuming that in the settling zone volume the volume fractions are equal to the volume fractions in the feed stream, then Eqs. (C.7) and (C.8) can be combined to obtain

$$-(v_z^s - v_z^f) = u_t(\epsilon_F^f)^b \tag{C.9}$$

By combining this with Eqs. (C.5) and (C.1), then Eq. (C.9) simplifies to

$$Q_L/A = u_t(\epsilon_F^f)^{b+1} \tag{C.10}$$

which indicates that for given u_t, b, and ϵ_F^f, the liquid overflow rate is specified. The assumption that the volume fraction in the settling zone is equal to the inlet condition is a "free settling" approximation (*6*) that allows for a tractable solution. Greater accuracy could be obtained using empirical models accounting for transient resistant effects (*7*) and entrance region effects. Models accounting for sludge funneling affecting the settling and compression zones could also improve upon the analysis (*8*) but are not considered here.

In the compression zone the material behavior is described by the momentum balances. Combining the two momentum balances, Eqs. (6) and (7), to eliminate the pressure term, and substitution of the constitutive relations, Eqs. (8) and (9), gives

$$-[B\mu A_s^2]\frac{\epsilon^{s2}}{(1 - \epsilon^s)^2}(v_z^f - v_z^s) + \sigma\frac{d\epsilon^s}{dz} + \epsilon^s(\rho^s - \rho^f)g = 0 \tag{C.11}$$

Substitution of Eqs. (C.5) and (C.6), rearrangemnt, and integration gives

$$\int_{\epsilon^s}^{\epsilon_c^s} \frac{d\epsilon^s}{[B\mu A_s^2]\dfrac{\epsilon^s}{(1-\epsilon^s)^2}\dfrac{Q_S}{A}\left[\dfrac{\epsilon_S^s - \epsilon^s}{(1-\epsilon^s)}\right] - \epsilon^s(\rho^s - \rho^f)g} = \frac{L - z}{\sigma} \qquad \text{(C.12)}$$

This expression can be numerically integrated to determine the local volume fraction as a function of local position from the top of the compression zone, $(L - z)$. However, this does not give the depth of the compression zone or the volume fraction of the sludge discharge. The volume fraction of the sludge discharge is important to determine the effectiveness of the thickeneing operation while the compression zone depth is needed for the design of the thickener.

With Q_F and ϵ_F^s given, then Q_S is obtained from Eqs. (C.1) and (C.10), and the sludge discharge volume fraction can be determined from the feed volume fraction with Eq. (C.2). Once the sludge discharge volume fraction is known, then the compression zone depth, L, is determined from the profile calculated with Eq. (C.12) for which by definition z is zero when ϵ^s is equal to ϵ_S^s.

On the basis of the material balances over the whole thickener, and the assumption that all solids exit through the sludge discharge, then Eqs. (C.1) and (C.2) can be combined and rearranged to obtain

$$Q_F = \frac{\epsilon_S^s Q_L}{(\epsilon_S^s - \epsilon_F^s)} \qquad \text{(C.13)}$$

where ϵ_S^s varies in the range $\epsilon_c^s \leq \epsilon_S^s \leq 1$ in the compression zone. Since Q_L is determined by Eq. (C.10), then Eq. (C.13) and the constraint on ϵ_S^s limit the allowable range of Q_F.

NOTATION

A	cross-sectional area of packed bed, filter cake, or thickener (m^2)
A_s	specific surface area between the phases (m^2/m^3)
B	parameter in Blake–Kozeny expression
b	parameter in hindered settling expression
$\mathbf{F}^d$, F_z^d	drag force between the phases, z-component (N/m^3)
g	gravity acceleration constant (9.807 m/s^2)
G	ratio of cake volume to filtrate volume, Eq. (B.3)
L	bed, cake, or sediment height (m)
M^s	total mass of solid materials in packed bed (kg)

P^f	fluid phase pressure (kPa)
P	piezometric pressure (kPa)
P_L, P_0	fluid pressure at positions $z = L$ and $z = 0$ (kPa)
ΔP	packed bed or filter cake pressure drop, $P_L - P_0$ (kPa)
Q	flow rate in packed bed or filter cake (m^3/s)
Q_F, Q_L, Q_S	feed, liquid overflow, and sludge discharge flow rates in thickener (m^3/s)
t	time (s)
u, u_t	hindered settling rate and terminal velocity (m/s)
v_z^f, v_z^s	fluid and solid phase mass averaged velocities (m/s)
W	pump power (watts)
ϵ^f, ϵ^s	fluid and solid phase local volume faractions (or concentration)
ϵ^s_{bed}	average volume fraction of packed bed
ϵ^s_{cake}	average volume fraction of filter cake
$\epsilon^s_{\text{slurry}}$	solid phase volume fraction of slurry above the filter cake
ϵ^s_F, ϵ^s_S	solid phase volume fraction of feed and sludge discharge streams
ϵ^s_0, ϵ^s_c	solid phase volume fraction at $z = 0$ and critical volume fraction
σ	modulus in solid phase stress-strain relation
$\boldsymbol{\tau}^s$, τ^s_{zz}	solid phase stress tensor and zz-component

REFERENCES

1. Anderson, T. B., and R. Jackson, "Fluid Mechanical Description of Fluidized Beds. Equations of Motion," *Ind. Eng. Chem. Fundam.*, *6*(4), 527 (1967).
2. Bear, J., *Dynamics of Fluids in Porous Media*, Elsevier, New York, 1972.
3. Bird, R. B., W. E. Stewart, E. N. Lightfoot, *Transport Phenomena*, Wiley, New York, 1960.
4. Chase, G. G., "Continuum Analysis of Constant Rate Cake Filtration," Ph.D. Dissertation, The University of Akron, Ohio, 1989.
5. Desai, F. N., "Balance Equations and Constitutive Equations for Porous Media Flows with Large Porosity Gradients," Ph. D. Dissertation, The University of Akron, Ohio, 1989.
6. Dixon, D. C., "Momentum-Balance Aspects of Free-Settling Theory. I. Batch Thickening," *Sep. Sci.*, *12*(2), 171 (1977).
7. Dixon, D. C., "Momentum-Balance Aspects of Free-Settling Theory. III. Transient Compression Resistance," *Sep. Sci. Technol.*, *13*(9), 753 (1978).
8. Dixon, D. C., "Thickener Dynamic Analysis, Accounting for Compression Effects," *Chem. Eng. Sci.*, *36*, 499 (1981).
9. Eringen, A. C., *Mechanics of Continua*, 2nd ed., Krieger, Huntington, New York, 1980.
10. Feda, J., *Mechanics of Particulate Materials: The Principles*, Elsevier, Amsterdam, 1982.
11. Hassanizadeh, M., and W. G. Gray, "General Conservation Equations for Multi-phase Systems: 1. Averaging Procedure," *Adv. Water Resour.*, *2*(3), 131 (1979).

12. Hassanizadeh, M., and W. G. Gray, "General Conservation Equations for Multi-phase Sytems: 2. Mass, Momenta, Energy, and Entropy Equations," *Ibid.*, *2*(4), 191 (1979).
13. Hassanizadeh, M., and W. G. Gray, "General Conservation Equations for Multi-phase Systems: 3. Constitutive Theory for Porous Media Flow," *Ibid.*, *3*(1), 25 (1980).
14. Hassanizadeh, S. M., and W. G. Gray, "Mechanics and Thermodynamics of Multiphase Flow in Porous Media Including Interphase Boundaries," *Ibid.*, *13*(4), 169 (1990).
15. Hutto, F. B., Jr., "Distribution of Porosity in Filter Cakes," *Chem. Eng. Prog.*, *53*(7), 28 (1957).
16. Maude, A. D., and R. L. Whitmore, "A Generalized Theory of Sedimentation," *Br. J. Appl. Phys.*, *9*, 477 (1958).
17. McCabe, W. L., J. C. Smith, and P. Harriott, *Unit Operations of Chemical Engineering*, 4th ed., McGraw-Hill, New York, 1985.
18. Murry, J. D., "On the Mathematics of Fluidization," *J. Fluid Mech.*, *21*(3), 465 (1965).
19. Purchas, D. B., *Solid/Liquid Separation Technology*, Uplands Press, Croydon, England, 1981.
20. Slattery, J. C. *Momentum, Energy, and Mass Transfer in Continua*, 2nd ed., Krieger, Huntington, New York, 1981.
21. Tiller, F. M., "The Role of Porosity in Filtration, Part 3: Variable-Pressure–Variable-Rate Filtration," *AIChE J.*, *4*(2), 170 (1958).
22. Whitaker, S., "Diffusion and Dispersion in Porous Media," *Ibid.*, *13*(3), 420 (1967).
23. Willis, M. S., R. M. Collins, and W. G. Bridges, "A Complete Analysis of Non-Parabolic Filtration Behavior," *Chem. Eng. Res. Des.*, *61*(2), 96 (1983).

Received by editor August 26, 1991